International Journal of Teknology Informatics and Engineering
e-ISSN :2961-8215;.p-ISSN :2961-9068
Volume 1 No. 3 , Desember - 2022

VIRTUAL SYNCHRONOUS GENERATOR-BASED OVERSIGHT AND PREDICTIVE MODELS FOR MARS

Migunani
Universitas Sains dan Teknologi Komputer

Moh Muthohir
Universitas Sains dan Teknologi Komputer

Dwi Setiawan
Universitas Sains dan Teknologi Komputer

Abstract. This research serves the virtual Synchronous Generator finding and oversight building of the Multi-port Autonomous Reconfigurable Solar (MARS) structure to bring backing to the alternating-curring network under various events on the network and presents a “model-based predictive control” (MBPC) oversight finding for the MARS structure to bring backing to the MARS structure alternating-curring network while the density innovation is recognized in the system. The main objective is to nominate a “model-based predictive control” leading oversight design that can bring density backing while unexpected density alteration. In this study, a comprehensive application of a virtual Synchronous Generator-based oversight innovation for the MARS structure is given. The expected oversight finding and control architecture of the MARS structure is evaluated by simulation on the “PSCAD”/EMTDC simulation platform to show performance under various operating conditions and calculated in the “Opal-RT” offline simulation model that also can be adapted to complete the certified “control-hardware - in-the- loops” (c-HIL).

The dominant density backing performance is a conceivable combined improvement for each current network-unified capability transistors system. By increasing infiltration of transistors system-based stuff, passivity and immediate density feedback potentially decrease. Leading “model-based predictive control” (MBPC) finding to provide density backing to current topologies of unified “photovoltaic” (PV), battery-based “energy storage system”s” (ESS), and “high-voltage direct current” (HVDC) method named “multi-port autonomous reconfigurable solar” (MARS) is suggested. The expected oversight finding for regularly based on virtual Synchronous Generator-based oversight. Simulation of the MARS-HVDC method by the recommended oversight approach was assumed and authorized for MARS related to a “small short circuit ratio” (SCR) network in a “PSCAD”/EMTDC assumed habitat. The expected oversight finding displays superior work in the phrase of increasing rock bottom frequency and increasing constant-area frequency concerning no density oversight.

The results of this research indicate that the MARS architecture by Synchronous Generator -based oversight brings exceptional heat backing by inserting higher active potential to the structure while equitable stage error compared to the Virtual Synchronous Generator - based oversight mode. The Synchronous Generator-based oversight mode is also balanced and brings better work in the phase of density rock bottom and balance-area increase. In the great feedback, the Synchronous Generator-based oversight mode is good than the Virtual Synchronous Generator-based oversight mode for each short circuit ratio set tested. MBPC-based oversight is entrenched in a virtual Synchronous Generator-based oversight algorithm. The recommended oversight innovation and control architecture of the MARS structure was calculated on the MARS structure in the "PSCAD"/EMTDC simulation environment. The simulation results show an increase in nadir frequency and steady-state frequency provided by the Multi-port Autonomous Reconfigurable Solar (MARS) structure via MBPC control. In future research, leading oversight methods are required to bring steady action down to unsteady error.

Keywords: Virtual Synchronous Generator, Photovoltaic, energy storage system, solar system, Reconfigurable Solar.

INTRODUCTION

Along with the increasing infiltration of "power electronic" shorted as "PE" but this PE is "based power plants", the inertia of the power network is decreased outcoming in current balanced threat. Grid-forming upturned that connect photovoltaic systems to grids and "energy storage systems"s" short as "ESS" is expected to hit an important model in appreciating this balancing issue. In addition, a "high-voltage direct current" (HVDC) link using the system will also make it possible to transmit the power from remotely placed photovoltaic power plants and to advanced grid balance. With increasing photovoltaic infiltration, the separate development of photovoltaic and power repository networks connected to alternating-current transmission networks and "high-voltage direct current" (HVDC) links is one of the solutions for stable network activity. Accordingly, a unified approach for the assimilation of photovoltaic and "energy storage system" to transmission alternating-curring network and "high-voltage direct current" (HVDC) link named a "Multi-Port Autonomous Reconfigurable Solar" (MARS) system is proposed. This research focuses on modeling, controlling, and implementing Multi-Port Autonomous Reconfigurable Sola systems. An advanced grid formation control method for Multi-Port Autonomous Reconfigurable Solar adopting classical and predictive control methods is proposed and compared with the following grid control method. A grid-factor controller is a controller that regulates the instantaneous terminal voltage of a power electronic (PE)-based converter with no "phase-locked loop" or shorted as "PLL" and might coexist with another "grid-forming", "grid-following", "Grid-synchronous" power sources within same "alternate current grid". A "grid-following" controller is a controller that estimates the instantaneous angle of the terminal voltage of a transistor system-based converter by helping phase-locked-loop and using a new oversight curve to determine the alternating-curring inserted into the alternating-curring grid. Additionally, a Multi-port Autonomous Reconfigurable Solar system is suggested as a possible explanation to mitigate the downtime issue shown in Power Electronic-based systems. The suggested solutions are compared with traditional approaches and modified.

"There is increasing significance in plan blended big-heat alternating-current/direct current (ac-dc) transmission systems (or hybrid transmission systems)" (Chinthavali et al., (2017)), "as the benefits bring by modular multilevel converters (MMCs)" (Barbosa et al., (2015). The development of integrated photovoltaic structures and "battery-based "energy storage system"s" is being marked at a faster step than previously as long as the associated techno-economic benefits. Following this development, a study on the assimilation of photovoltaic and power repository networks to "high-voltage direct current" shortened as "HVDC" is becoming popular recently. In this area, the development of an integrated photovoltaic and power repository system connected to an “alternating-current” (ac) transmission network and big-heat system explicitly present through a “multi-port autonomous reconfigurable solar plant” or MARS is given in this study. Another thing that the increasing infiltration of the transistors system in networks is a decrease in the network's ability to repair by the heat (voltage) or density (frequency) confusion. Advanced oversight action in transistor system systems and the use of the “ac-dc” hybrid method might improve the balance of the power network (grid). This research serves a virtual Synchronous Generator-based oversight finding in a “Multi-Port Autonomous Reconfigurable Solar” system that can enhance the ability of the grid to return to the density explosion. The oversight finding can bring density backing while workout on the grid that matter regularity confusion. On the other side, to density backing, the expected oversight finding brings voltage base in the event of an equitable fault and establishes no outage of service. Typically, service outages can be recognized in historical photovoltaic generators or “energy storage system”s due to voltage drop/increase or changeable regularity as these work. The stratified control structure of the “Multi-port Autonomous Reconfigurable Solar” or shorted the “MARS” system that is presented here can back a virtual Synchronous Generator-based control design.

“Simulation research to classify the performance of the advanced Multi-port Autonomous Reconfigurable Solar (MARS) control architecture and the virtual Synchronous Generator algorithm” (Weiss et al., (2011); Sheng et al., (2014)) “covered by different analysis cases and extreme operating conditions were performed on the “PSCAD” simulation software” (Molinas et al., (2017); Amin et al., (2016)). “The proposed design is related to the Virtual Synchronous Generator (VSG) oversight” (Tonkoski et al., (2017); Visscher et al., (2009)) The oversight mechanism and the benefits of the advanced oversight design compared to the Virtual Synchronous Generator based oversight mode is granted. The correlation particularly serves for the relation of the MARS structure to a powerless, low-inertia network, that is normal to grow by increasing infiltration of transistors system-based resources in the network. The oversight algorithm was calculated in an offline Opal-RT simulation, and the advanced model might be adopted for advanced “hardware-in-the-loop” (c-HIL) control device simulations in the future.

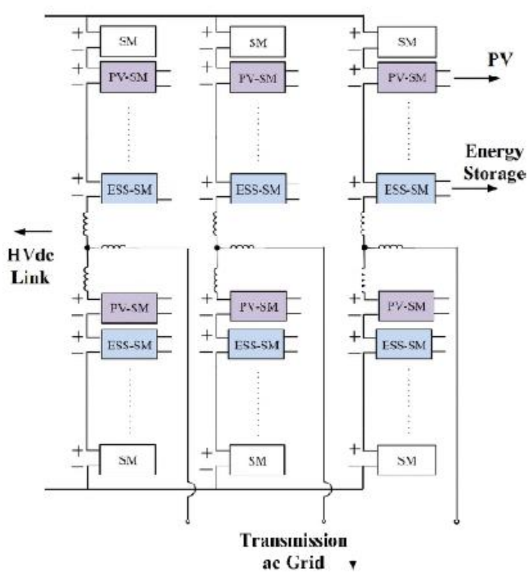

Figure 1a. Synopsis of the MARS building structure

One of the concerns with transistor system-based systems with the integration of renewable energy is the reduction in overall "grid inertia" because transistor system-based networks have no physical inertia compared to conventional power systems. Amplifying the system by virtual inertia through leading oversight methods is one of the answers to stabilize the network in case of regularity-related events. The main objective of this study is to propose a "model-based predictive control" (MBPC) leading oversight scheme that can provide regularity support during unexpected density alteration. Compared to conventional control methods, "model-based predictive control" was chosen for regularity support because of this essential benefit as long as the formation of pressure, prediction of the system state, and better dynamic performance (Cortes et al., (2012)). The proposed MBPC-based oversight mode is part of a new transistors system resource-based system called "Multiport Autonomous Reconfigurable Solar Plants" (MARS). The MARS structure is an integrated development for an "energy storage system" (ESS) photovoltaic and battery-based "energy storage system" (ESS) linked to "alternating-current" (ac) and "high-voltage direct current" (HVDC) transmission networks (Figure 1a).

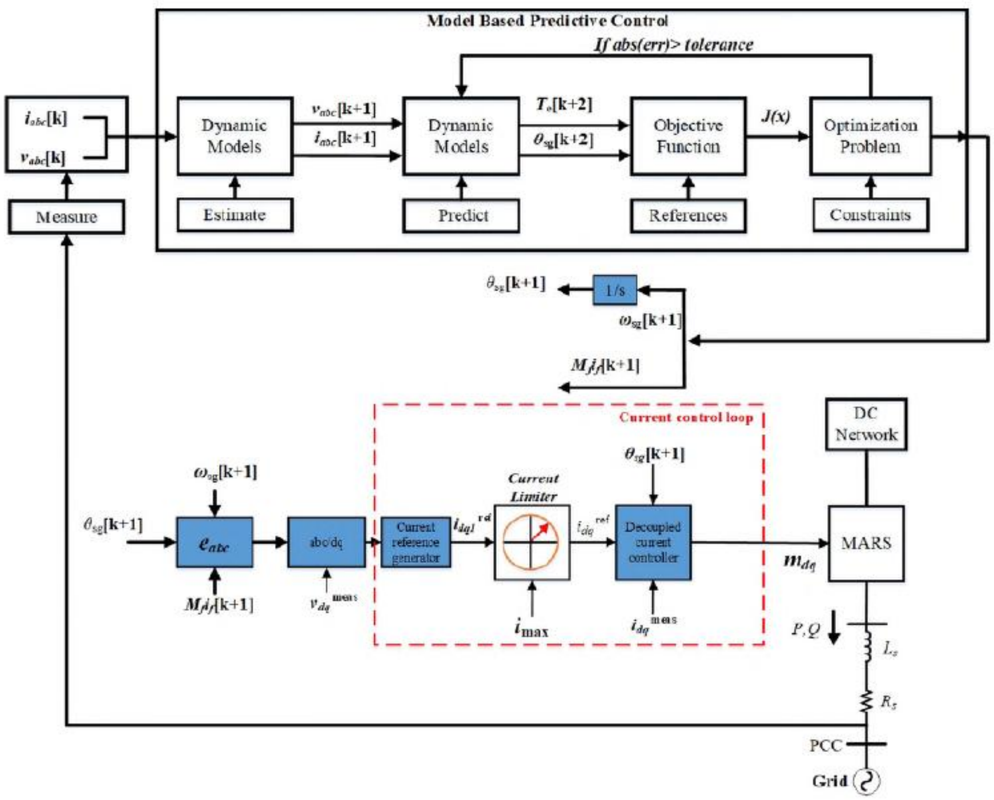

Figure 1b MBPC-based oversight for the MARS structure

The MARS structure oversight structure is hierarchical and deeply complicated. It subsists of 3 layers with various functions. First, the top-balanced controller (L-1) combines effective energy oversight, sensitive energy oversight control, "model-based predictive control" (MBPC) density oversight, alternating-curring "side-voltage-control", and "dc" (direct current) "side-voltage-control". The 2^{nd} is, the middle-level controller (L-2) includes quantification voltage steadying control and a cumulative "energy storage system" (ESS), and PV power control. Finally, low-level control (L-3) consists of "maximum power point tracking" shorted as "MPPT" control for photovoltaic submodules (SM) and “state of charge” (SoC) control for “energy storage system” Sub Modules. In this study, a “model-based predictive control” (MBPC)-based oversight mode is proposed for regularity support on the L-1 controller. Virtual Synchronous Generators emulate the property of synchronous generators subject to regularity backing and voltage backing. The regularity and voltage models adopted in the MBPC-based oversight mode objective function are rolled on the synchronous alternator role. The suggested optimization issues fixed the corner regularity (ω_{sg}). The suggested control structure was tested on a leading large-loyalty 3-phase Autonomous Reconfigurable Solar Multi-port system model that utilizes an ultra-fast simulation algorithm connected to a reduced-order alternating-curring grid model. The effectiveness of the expected oversight finding was certified and calculated for each certified fact in the “PSCAD”/EMTDC simulation environment.

LITERATURE REVIEW

MARS structure Model

An overview of the Multi-port Autonomous Reconfigurable Solar (MARS) system architecture is shown in Figure 1a, it has 6 wings (hand) in total, with different wings divided into normal N_{norm} (SM) submodules, N_{pvPV} -SM_s, and N_{ess} “energy storage system” (ESS)-SMs. Normal SMs are based on ½ bridges, that also the front end of photovoltaic and “energy storage systems”s (ESS-SMs). The photovoltaic system in PV-SM is linked to the frontal point by a uni-directional dc-dc converter. The “energy storage system” (ESS) system in the “energy storage system” (ESS)-SMs is linked to the frontal point by a 2-step “dc-dc converter”. The mathematical modeling is based on methods identical to the modular multilevel converters (MMC) mathematical modeling described in.

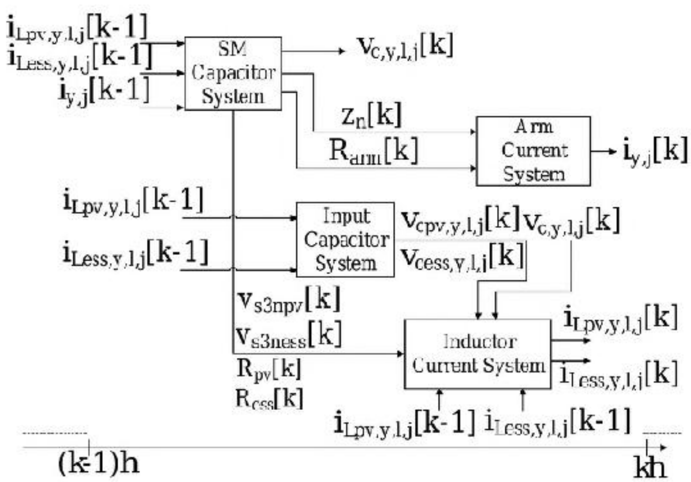

Figure 2. MARS simulation algorithm

Reflection of the “MARS” structure on classical reflection way is time-exhausting and expensive. Thus, it is very important to adopt the progressive system and quick duplication design to certify the oversight architecture of the MARS structure. The advanced MARS structure role is characterized by “differential-algebraic equations” or shoted as “DAE” and separated occupying the binary rigor in the differential algebraic equations section. The separate network is then discretized based on their affected rigidity setting to cut down the required computing complication. A complete brief of the duplication finding to affect the MARS structure is illustrated in Figure 2.

MARS stratified Oversight Structure

The MARS oversight network (Figure 3) includes “controller L-1”, “controller L-2”, and “controller L-3”. The functionality of the L-1 controller includes voltage and regularity support to the grid, operation and reactive power control, dc-link voltage control, ac-/dc side current control, and energy steady between each class of SMs (photovoltaic, “energy storage system” (ESS), and ordinary). Voltage and regularity support in the L-1 controller is based on a Synchronous Generator-based oversight algorithm that regulates the rotor angle (θ_{sg}), corner regularity (ω_{sg}), and system output voltage MARS three e_{ABC}. The L-1 controller also determines the reference power commands of the PV and “energy storage system” (ESS) in the MARS structure ($P_{PV.ref}$, ref and $P_{ess, ref}$). Reference power commands from PV and “energy storage system” (ESS) depend on power delivery commands ($P_{ac, ref}$, $P_{dc, ref}$, and $Q_{ac, ref}$), power requirements of Synchronous Generator-based oversight, maximum available PV power ($P_{PV,mppt}$), and the SM “energy storage system” rating ($P_{ess, rating}$). The active and reactive power references on the alternating-curring side of the MARS structure are the sum of the corresponding sending commands and the corresponding power requirements of the Synchronous Generator-based oversight. Based on the determined θ_{sg}, $\bar{\omega}_{sg}$, and e_{abc}, the control current *qd* of the alternating-curring side current is calculated to generate the modulation index m_{abc}.

The power setting control produces a mention moving present in the stage leg which is controlled by the moving-present control to produce $m_{circ,abc}$. Circulation presents control consisting of the 1st, 2nd, and 4th harmonics which are controlled by adopting the “*qd transformation*” based on (Chinthavali., (2016)). During the 1st harmonic is controlled based on the resulting power balance control reference, the 2nd and 4th harmonics are controlled to zero. The modulation indices $m_{circe, abc}$, and m_{abc} are combined to produce a wing inflection index $m_{abc}^{p,n}$ based on (Chinthavali., (2016)). The L-1 controller sends each arm’s inflection index, PV reference power, and “energy storage system” reference power to the L-2 controller. The L-2 controller maintains the capacitor voltage and also generates a switching signal for the front-end half-bridge of all SMs based on (Chinthavali., (2016)). The L-3 controller controls the power from the PV and the SM “energy storage system” controls the current of the dc-dc converter and sends switching commands to the dc-dc converter.

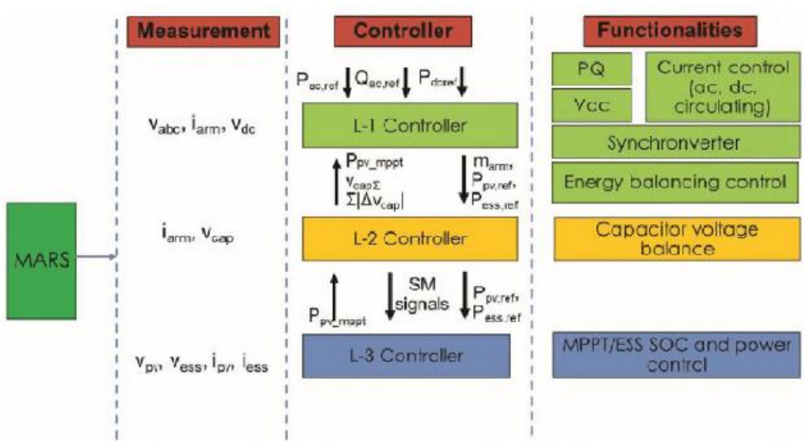

Figure 3. MARS Control Architecture

“Virtual Synchronous Generator” Based oversight finding

The Synchronous Generator-based oversight design placed in the MARS structure oversight network is shown in Figure 4. This algorithm consists of ruler loops, inertial loops, reactive power loops, active power loops, and current control loops. The ruler model is a time constant T_D with gain D_{p1}. The time-constant $_{TD}$ of the ruler delay is used to simulate the mechanical response delay of a synchronous generator's physical ruler. The term D $_{pi}$ is regularity - power drop coefficient. The upper limit of active power (P_{max}) is the maximum power available at that time that can be used (i.e. the sum of $P_{de,\ ref}$, $P_{pv,\ moot,}$ and $P_{ess,\ rating}$). The lower limit of active power (P_{min}) is the minimum power available at that time that can be used (i.e. the sum of $P_{dc,\ ref,}$ and $P_{ess,\ rating}$ (used for charging). The ruler control mechanism shown in Figure 4 can be expressed in the Laplace domain as

$$P_{\text{gov}}(s) = \frac{D_{pI}}{(1 + T_{Ds)}} (\omega_n(s) - \omega_{sg}(s))$$

where m_n is the mentioned corner regularity mention and ‘ω_{sg} is the corner regularity determined from the Synchronous Generator-based oversight. During the ruler control depiction in the ‘Laplace domain’, the application executes in the time domain by discretizing adopting the forward-Euler method.

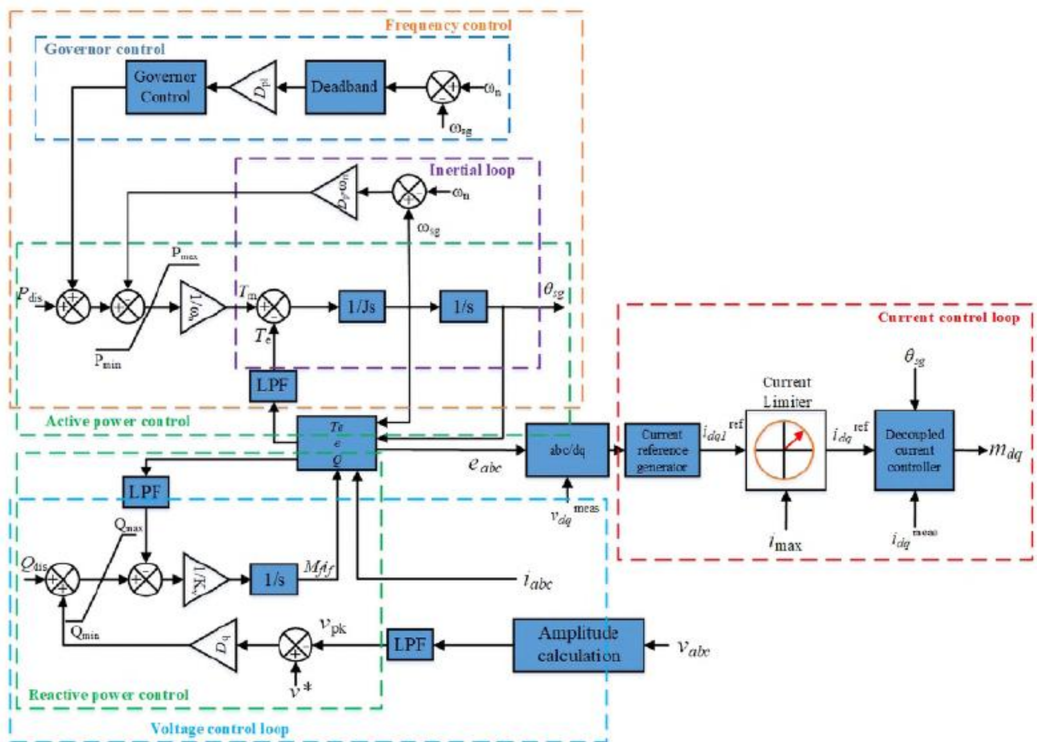

Figure 4. Virtual Synchronous Generator-based oversight algorithm

“Inertial loop”, “active power loop”, and “reactive power loop” are based on the virtual Synchronous Generator approach definite in research by Weiss et al., (2011). The electromagnetic torque T_e, the 3-step system outcome heat of MARS e_{abc}, and the sensitive energy Q are addicted as follows:

$$T_e = M_f i_f < \boldsymbol{i}, (\widetilde{\boldsymbol{cos(\theta)}}) >,$$
$$e_{abc} = \dot{\theta} M_f i_f (\widetilde{cos(\theta)}),$$
$$Q = \dot{\theta} M_f i_f < \boldsymbol{i}, (\widetilde{\boldsymbol{sin(\theta)}}) >,$$

Where is the factor $\mathbf{i}$, $\widetilde{\cos(\theta)}$, $dan\ \widetilde{\sin(\theta)}$.the reference current generator adjust the structure hint current *qd* based on the lap equation that makes use of each the voltage 'e_{abc}' and the "ac-side" heat v_s. The discrete lap equation adopted to calculate the reference current structure abc is adopting the "backward-Euler" system. "By calculated *abc reference current frame, the qd reference current frame is* calculated based on Park's revolution" given in research by Pekarek et al., (2013):

$$i_a[k] = \frac{i_a[k\ 1] + \frac{h}{L_s = L_o/2} \times (e_a[k] - v_a[k])}{\left(1 + h \times \frac{R_s + R_o/2}{L_s + L_s/2}\right)}$$

$$i_b[k] = \frac{i_b[k-1] + \frac{h}{L_s + L_s/2} \times (e_b[k] - v_b[k])}{(1 + h \times \frac{R_s + R_o/2}{L_{s+L_s}/2})}$$

$$i_c[k] = \frac{i_c[k-1] + \frac{h}{L_s + L_{o/2}} \times (e_c[k] - v_c[k])}{(1 + h \times \frac{R_s + R_o/2}{L_o + L_o/2})}$$

'L_o' and 'Ro' is the conscience of the wings and the defiance of the wings are network (grid) that conscience and network support appropriately, h is the duplication season stage. Since the Synchronous Generator-based oversight is mainly instrumented as a heat authority instrumentation, it does not have over-current limit conservation. Nonetheless, a present limiter is given to limit the overcurrent in the network. The separated present controller comprises a qd control of the alternating-curring side current that produces the appropriated inflection index. Theta (θ_{sg}) is determined by the Synchronous Generator-based oversight adopted in the circulation flow oversight and "*qd current control*".

MBPC

The square chart by a "model-based predictive control" (MBPC) virtual Synchronous Generator control is shown in Figure 4, consists of a dynamic model to estimate and conclude the system state, an equitable function to convert the control objectives into scalar cost values, and an optimization problem to minimize the equitable function. The "MBPC"-based virtual Synchronous Generator control idea is to produce the optimal $\omega_{sg\ value}$ by minimizing the equitable objection. Details about different squares are given in the following area.

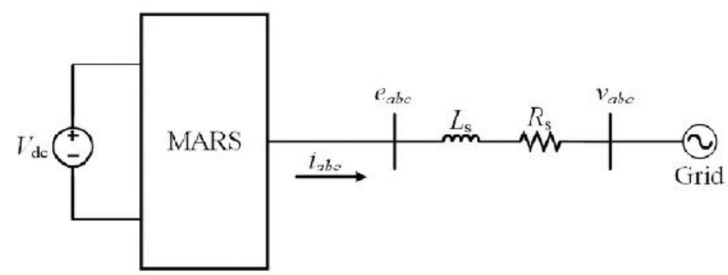

Figure 5. MARS particular line chart linked to the network (grid)

Standard Establishment

Private Progressive Standard of MARS-HVDC.

The particular line chart of the network-linked MARS structure serve in Fig.5. The MARS structure is a 3-step method with a total of 6-arms which integrates photovoltaic and "energy storage system"s using transistors system and might be linked to “HVDC” and high heat-transmission of alternating-curring network voltage. Each wing includes the normal ‘SM’, photovoltaic, and “energy storage system”. SM together with wing Lo and wing resistance (*Ro)*. The PV system in each photovoltaic-SM is connected to the SM by hidden or non-hidden “dc-dc” converters. The “energy storage system” in each “energy storage system” -SM is linked via a two-way dc-dc proponent. Various converter phase is connected to the utility network via array RL branches. The dynamic continuous time scheme and the various-time mechanism of the MARS structure were developed based on the discretization of the continuous time model. The advanced various model is adopted in the automated implementation of the MBPC method. A schematic of the equivalent decreased-regulation MARS scheme structure serve in Figure 6.

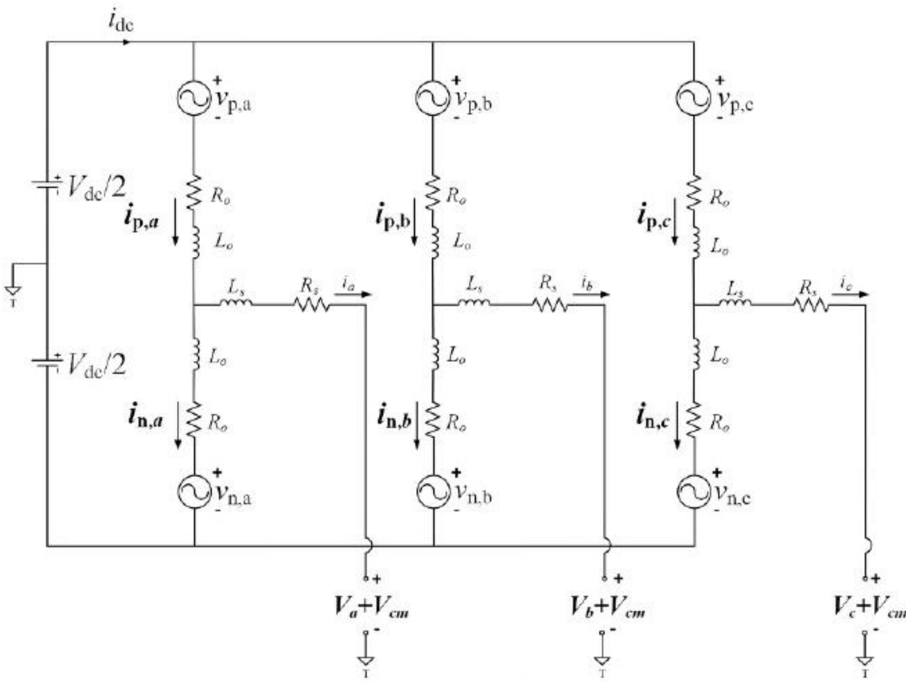

Figure 6. Schematic of the MARS reduced model

The wing at top of $v_{p,j}$ and the lower wing $v_{n,y}$ *of the* j - phase:

$$v_{p,j} = V_{dc} - L_o \frac{di_{p,j}}{d_t} - R_p i_{p.j} - L_s \frac{di_j}{dt} - R_s i_j - v_j - v_{cm}, \forall j \in (a,b,c),$$

$$v_{n,j} = V_{dc} - L_o \frac{di_{n,j}}{dt} - R_o i_{n,j} + L_s \frac{di_j}{dt} + R_s i_j + v_j + v_{cm1}, \forall j \in (a,b,c),$$

where V_{dc} is the heat, and $v_{cm1} = v_{cm} - V_{dc}$; $I_{p,j}$ and $i_{n,j}$ is the upper wing and lower wing currents

The dynamic continuous time model of the MARS structure shown in Figure 7 is given by (1) and obtained by adding (1a) and (1b) with the following assumptions: (i) the SM capacitor voltage is balanced; and (ii) the common mode voltages (v_{cm} and v_{cm1}) are ignored:

$$(L_s + L_o/2)\frac{di_j}{dt} + (R_s + R_o/2)i_j = e\,j - v\,j, \forall\, j\ \in (a,b,c)$$

where i is the 3-step network current; vy is the 3-step network voltage, and the 3-step outcome heat (e_{j}) of the MARS structure is

$$ej = \frac{-v_{p,j} + v_{n,j}}{2}, \forall\, j \in (a, b, c)$$

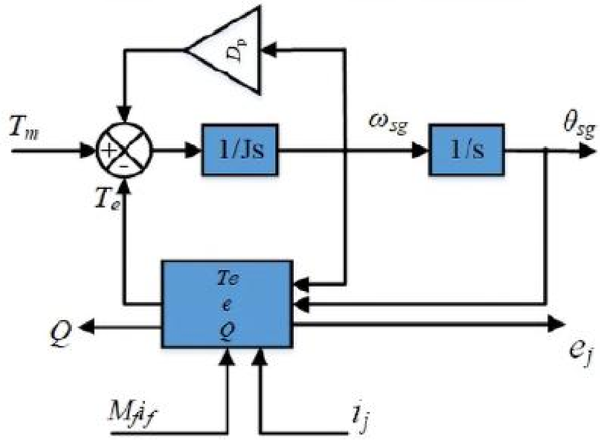

Figure 7. Virtual Synchronous Generator control block

The discrete-duration role of the MARS structure is obtained by discrete (1) using the forward-Euler method and is given by:

$$i_a[k] = \left(1 - h\frac{R_s + R_O/2}{L_s + L_o/2}\right)(i_a[k-1]) + \frac{h}{L_s + L_s/2}(e_a[k-1] - v_a[k-1])$$

$$i_b[k] = \left(1 - h\frac{R_s + R_O/2}{L_s + L_o/2}\right)(i_b[k-1]) + \frac{h}{L_s + L_o/2}(e_b[k-1] - v_b[k-1])$$

$$i_c[k] = \left(1 - h\frac{R_s + R_O/2}{L_s + L_s/2}\right)(i_c[k-1]) + \frac{h}{L_s + L_s/2}(e_c[k-1] - v_c[k-1])$$

where 'h' is the simulated time stage and 'k' is the instantaneous time.

Virtual Synchronous Generator-Based Frequency Model

The density model is stationed on the synchronizer model. "Virtual Synchronous Generators mimic the property of synchronous generators in providing frequency support and voltage support during grid events that cause the density or voltage deviations" (Weiss et al., (2011)). A virtual Synchronous Generator-based oversight block is derived using a mathematical model of a roto synchronous generator. "The discrete-time representation of the electromagnetic torque (T_{e}), ey, and reactive power (Q) is given in a three-phase integer" (Weiss et al., (2011)) and shown in Figure 7.

$$T_e[k] = M_f i_f[k](i_a[k]\ \cos\ (\theta_{sg}[k]) + i_b[k]\cos(\theta_{sg}[k] - 2\pi/3) + i_c[k]\cos(\theta_{sg}[k] - 4\pi/3))$$

$$e_a[k] = \omega_{sg}[k] M_f i_f[k] \cos(\theta_{sg}[k])$$

$$e_b[k] = \omega_{sg}[k] M_f i_f[k] \cos(\theta_{sg}[k] - 2\pi/3)$$

$$e_c[k] = \omega_{sg}[k] M_F i_f[k] i_a[k]\, sin(\theta_{sg}[k] - 4\pi/3)$$

$$Q[k] = -\omega_{sg}[k] M_f i_f[k] i_a[k] \sin(\theta_{sg}[k]) + i_b[k]\sin(\theta_{sg}[k] - 2\pi/3 + i_c[k]\sin(\theta_{sg}[k] - 4\pi/3)$$

"where $M_f i_f$ in (4) is the oversight input to the virtual Synchronous Generator" (Weiss et al., (2011)). In Figure 7, θ_{sg} determined as

$$\theta_{sg}[k] = \theta_{sg}[k-1] + h\omega_{sg}[k-1]$$

The effectiveness of the network regularity is characterized by the discrete-time role represented by:

$$\omega_{sg}[k] = \omega_{sg}[k-1]\left(1\frac{h\mathrm{D}p}{J}\right) + \frac{h}{J}(T_m[k] - T_e[k] - D_p(\omega_n[k]))$$

"Virtual Synchronous Generator" Based oversight

"The suggested Synchronous Generator-based system was compared with a "VSG"-based oversight" (Tonkoski et al., (2017)). The L-1 controller uses a "VSG"-based oversight mode to regulate the active and reactive power commands based on the rated "ac-side" voltage from the MARS structure (v_{abc}). The alternating-curring side voltage of the MARS structure is processed by a phase-locked loop (PLL) to regulate the peak value and regularity of the voltage (v_{pk} and f). The peak value and regularity are used subsequently to define other belly floors combined with the transmitted operation and affective energy commands.

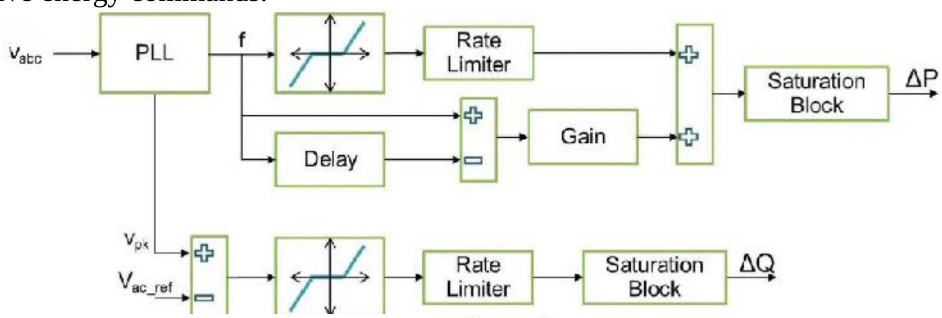

Figure 8. "VSG" based oversight

Equitable Objection

The equitable objection based on the discrete-time model is:

$$\min_{x} J(x)$$

$$s.t \quad \boldsymbol{e}[k=1] = \omega_{sg}[k=1]\mathrm{M_f i_f}[k](cos(\theta_{sg}[\widetilde{\boldsymbol{k}+\boldsymbol{1}}]))$$

$$\theta_{sg}[k+1] = \theta_{sg}[k] + h\omega_{sg}[k]$$

$$T_e[k+2] = M_f i_f[k] < \boldsymbol{i}[k+\boldsymbol{2}], (\boldsymbol{cos}(\boldsymbol{\theta_{sg}}[\widetilde{\mathbf{k}-\mathbf{2}}])) >;$$

$$T_m[k+2] = \frac{P_{ac,ref}[k+2]}{\omega_n[k+1]};$$

Where 'x' and '$J(x)$' are:

$$x = (\omega_{sg}[k+1])^T$$

$$J(x) = J_1(x) + J_2(x)$$

Where

$$J_1(x) = \lambda_1(T_e[k+2] - T_m[k+2])^2$$

$$J_2(x) = \lambda_2(\omega_n[k+1] - \omega_{sg}[k+1])^2$$

"where λ_1, and λ_2 are the weights of the cost function; $P_{ac,\ the\ ref}$ is the alternating-curring side power delivery command; and vector **i**, cos(θ), and sin(θ)" are described in the study by Weiss et al., (2011).

SIMULATION RESULTS & VALIDATION

Implementation of the Proposed Control Method

i_j and v_j are measured from the alternating-curring grid model used in the simulation at $[k]^{th}$. After i_j is measured at $[k]$, using the dynamic model in (3) ij_{at} $[k+1]^{st}$ is estimated. Since the variation of v_j is slower than the dynamics of the MARS structure, in this implementation v_j at times $[k+1]^{st}$ is assumed to be the same as v_j at $[k]$ times.

Unlimited Development

The cost function J (x) is minimized using the Newton method described in (Zak et al., (2004)). The message ω_{sg} [k + 1] at each time phase is determined by:

$$x[k+1]^{(n+1)} = x[k+1]^{(n)} - F\left(x[k+1]^{(n)}\right)^{-1} g[k+1]^{(n)}$$

Where

$$F\left(x[k+1]^{(n)}\right) = \left[\frac{\partial g[k+1]^{(n)}}{\partial x[k+1]}\right]; g[k+1]^{(n)} = \left[\frac{\partial J(x[k+1]^{(n)}}{\partial x[k+1]}\right];$$

Testing System

Assuming one hundred and fifty kilowatts, one kilovolt of photovoltaic, and "energy storage system" SM, the number of SM per wing is 111 photovoltaic, thirty-seven "energy storage system"s, and 81 SM_s Normal. The size of the SM_s PV and "energy storage system" was determined based on the use of a 200 A, 3.3 kV SiC device in a dc-dc converter. The total number of SM_s per wing is determined by the dc-link voltage at the installation site and based on the installed "HVDC" substation (in the Transbay Cable project).

MARS structure with the Grid- alternating-curring Model

The alternating-curring grid in "WECC" is created based on "WSEIG1" to precisely serve as available density information. The comprehensive MARS structure model developed was tested for various low "short circuit ratio" network situations and low inertia conditions. "MARS structures based on traditional control methods are very vulnerable to weak network conditions for the following reasons" (WECC, (2014)):

1. The MARS structure has no inertia because there is no rotating mass.
2. Electronic control relies on a balanced voltage hint by the network to give operation and active power.
3. As the network turns powerless, oversight spec can influence the network behavior.

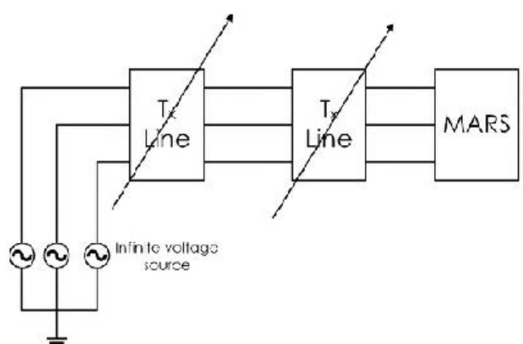

Figure 9. Setup of the simulation model for the low "SCR" Test

To overcome this problem, the suggested leading oversight is designed to establish the strong process of the "MARS" structure in these unsteady networks. To certify the improvement of the suggested controller, the "MARS" structure was certified during each "SCR" and 'low inertia' status. There are many systems for measuring network power. The other way to present the network power of a power system is with "SCR" because the analysis of the strong network is relevant to the identical impedance drawn by the terminal of the MARS structure to the power system. Then, to imitate a highly sustainable infiltration network with a small "SCR", the transmission line among the MARS structure and the alternating-curring network method is mixed. The transmission line lengths for each "SCR"s serve in Table 1. Two other facts were identified and tested for operating conditions P_{ac} as P_{dc} is one hundred megawatts for "SCR" facts is zero point five, two, four, and ten.

SCR	Resistance (Ω)	Inductance (H)	Line Length (km)
0.5	14.369	0.6715	861.5
2	3.5535	0.1661	198
4	1.7547	0.0820	87.65
10	0.6333	0.0296	18.85

Table 1. "SCR" ratio for different line lengths

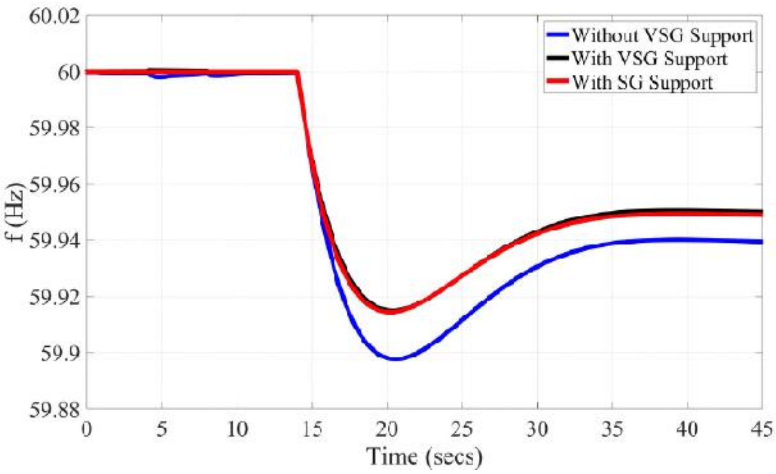

Figure 10. Grid Regularity feedback for "LOG" at "WECC" for "SCR" is ten

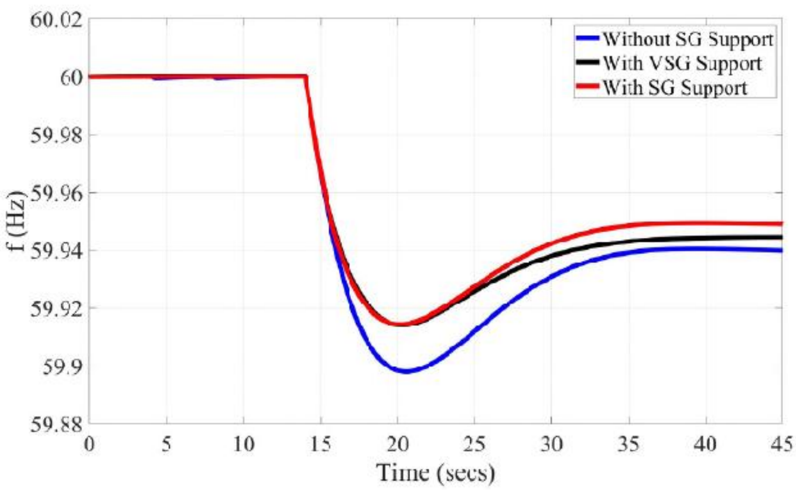

Figure 11. Grid Regularity feedback for "LOG" at "WECC" for "SCR" = is fo

An 804,44 megawatts "LOG" (loss-of-generation) event at "WECC" was assumed the t is fourteen seconds. The measured regularity responses for the various "SCR" facts with no base, with 'SG' base, and "VSG" base by the MARS structure serves in Figure 10 - 13. On an active grid with a high "SCR", the frequency support provided by the MARS structure over the "VSG" control method is greater than the frequency support provided by the MARS structure through the SG control method as illustrated in Figure 7. As the power of the system decreases in terms of "SCR", the frequency support provided by the MARS structure through the Synchronous Generator-based oversight mode is higher than the regularity base given by the MARS structure through the "VSG"-based oversight mode. That incident can check in Figure 10 - Figure 13, the reason for that is, the "VSG"-based oversight mode is armed by a slower controller. The "VSG"-

based oversight mode consists of a frequency-derived phrase and its analysis over the phase-locked loop is especially challenging in weak networks. The active “VSG”-based oversights with quick controllers may cause the vibration that may start to volatile the process due to this secondary regular term. Thus, the “VSG” controller must be managed by the passive controller. This issue is not visible in the Synchronous Generator-based oversight, because this system does not have the terms phase-locked loop and derivatives. The frequency increase in rock bottom and regular-area conditions for different “SCR” statuses and a different class of authority is sequential in Table 2.

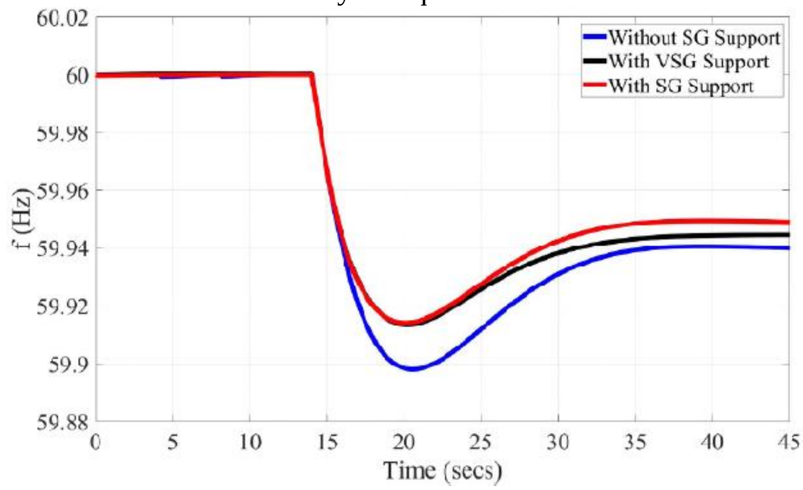

Figure 12. Grid Regularity feedback for “LOG” at “WECC” for “SCR” is two

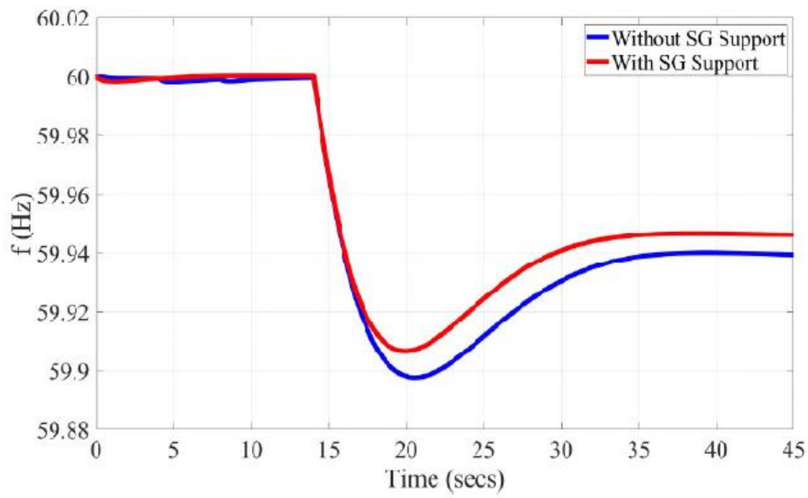

Figure 13. Grid Regularity feedback “LOG” at “WECC” for “SCR” is zero point five

SCR	Improvements			
	SG		VSG	
	nadir	steady state	nadir	steady state
0.5	8.69 %	11.00 %	UNSTABLE	
2	15.75 %	15.07 %	15.05 %	7.67 %
4	16.04 %	15.18 %	15.72 %	7.81 %
10	16.37 %	15.66 %	16.87 %	17.34 %

Table 2. Enhanced regularity feedback for each “SCR”s

3-phase faults are simulated on the sending line among the grid and the “MARS” structure when t is zero point four seconds by an error period of zero point two seconds. After zero point two seconds, the error clears itself. The improvement of the a-phase voltage profile with the help of “VSG” supports and SG supports while faults in each“SCR” setting (Figure 11 - Figure 13, and Table 3).

SCR	Improvements	
	SG	VSG
0.5	STABLE	UNSTABLE
2	21.25 %	17.21 %
4	14.16 %	10.98 %
10	6.81 %	5.33 %

Table 3. Improved voltage response for different “SCR”s

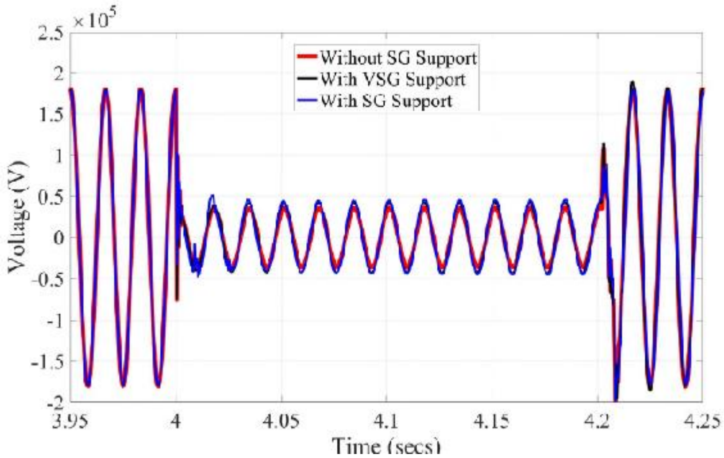

Figure 14. Phase-voltage profile for 3-step error “SCR” is ten

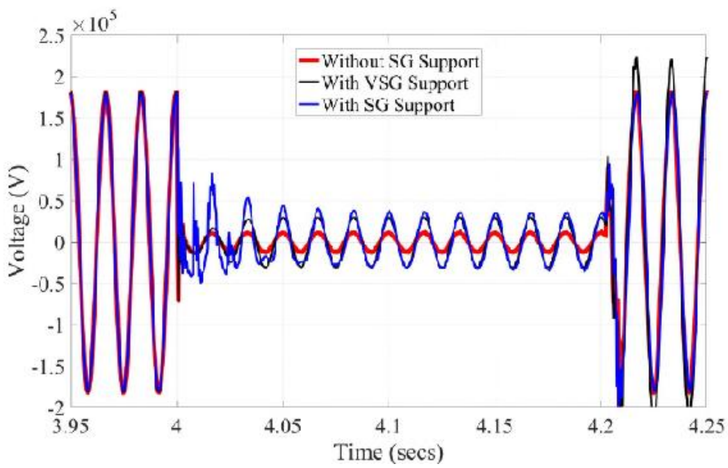

Figure 15. The step-voltage line for 3-error steps for “SCR” is four

Considering each “SCR” fact, the voltage base given by the MARS design over the Synchronous Generator-based oversight mode is bigger than the voltage base that is given by the MARS structure through the “VSG”-based oversight mode. Nevertheless, when “SCR” is in ten, the operating power given by the Synchronous Generator-based oversight mode is smaller than the “VSG”-based oversight mode (Figure 16). A passive controller is adopted in “VSG”-based oversight implementations due to the phase-locked loop analysis being very receptive to modification in grids. This outcome is a wrong estimate of the size of the “ac-side” summit heat. Thus, the comparable domination advance adopted in operating power controllers is decreased to establish that the supplementary sensitive power is unconcerned by vibration popularized in defective summitvoltages.

CONCLUSIONS AND RECOMMENDATIONS

This research provides the “VSG” design and oversight structure of the Multi-port “Autonomous Reconfigurable Solar” system to give support to the alternating-curring network under various events on the network and presents a “model-based predictive control” oversight finding for the MARS structure to give backing to the MARS structure. alternating-curring network during density modifications is detected in the network. A proposed Synchronous Generator-based oversight algorithm to support alternating-curring network frequency and voltage during network disturbances. In other that, a concise characterization of the global oversight construction of the MARS structure is given. The expected oversight finding and MARS oversight structure were calculated and authorized for the MARS structure in a “PSCAD” or “EMTDC” simulation area. The “OPAL-RT” offline simulation model appropriate to operate hardware-in-the-loop (c-HIL) control tests were also developed. The developed model and the expected oversight finding are certified for each grid scheme. To recap the outcomes, for the explicit research method studied in this study, the MARS structure by Synchronous Generator-based oversight provided good density backing in the scope of high-density rock bottom and higher density balanced area while density expedition compared to the control-based “VSG” mechanism. The MARS structure by Synchronous Generator-based oversight gives good heat backing by injecting higher conscious power into the mechanism while equitable error step compared to the “VSG”-based oversight mode.

An important point that can be drawn from this research effort as each study system studied deeply in this research, the Synchronous Generator-based oversight mode is highly balanced and provides a good function in terms of rock bottom density and balance-area advancement. For the heat feedback, the Synchronous Generator-based oversight mode is more good than the “VSG”-based oversight mode for each “SCR” condition tested. MBPC-based oversight is fixed to a “virtual Synchronous Generator”-based oversight structure. The expected oversight finding and control architecture of the MARS structure was evaluated on the MARS structure in the “PSCAD”/EMTDC simulation environment. The simulation results show an increase in nadir frequency and steady-state frequency provided by the Multi-port Autonomous Reconfigurable Solar (MARS) system via MBPC control. Virtual Synchronous Generator performance during unbalanced faults is an avenue of research that has not been explored and still raises open questions (Shen et al., (2017)). Other another main threat when the error is unstable is capturing the dynamics of the fastly changing alternating-curring side voltages. The inefficiency to precisely take “ac-side” heat dynamics outcomes in unnatural “ac-side grid” present. Leading oversight methods are required to bring the balanced operation down the unbalanced errors.

BIBLIOGRAPHY

EKP Chong and SH Zak, An Introduction to Optimization. Wiley, 2004.

H. Knaak, "Modular multilevel converters and HVDC/FACTS: A success story," in Proc. 201114th European Conference on Transistors system and Applications, pp. 16.

H. Knaak, "Modular multilevel converters and HVDC/FACTS: A success story," in Proc. 2011 14th European Conference on Transistors system and Applications, pp. 1-6.

J. Rodriguez and P. Cortes, Predictive Control of Power Converters and Electrical Drives. Wiley-IEEE Press, 2012.

M. Amin and M. Molinas, "Self-synchronization of wind farm in MMC-based HVDC system," in Proc. 2016 IEEE Electrical Power and Energy Conference (EPEC), pp. 16.

M. Amin, A. Rygg, and M. Molinas, "Self-synchronization of wind farm in an MMC-based HVDC system: A stability investigation," IEEE Transactions on Energy Conversion, vol. 32, no. 2, pp. 458-470, 2017.

MPN Van Wesenbeeck, SWH De Haan, P. Varela, and K. Visscher, "Grid-tied converter with virtual kinetic storage," in Proc. 2009 IEEE Bucharest PowerTech, pp. 1-7.

P. Krause, O. Wasynczuk, S. Sudhoff, S. Norrga, and S. Pekarek, Analysis of Electric Machinery and Drive Systems. Wiley-IEEE Press, 2013.

Q. Zhong and G. Weiss, "Synchroverter: Inverters that mimic synchronous generators," IEEE Transactions on Industrial Electronics, vol. 58, pp. 1259-1267, Apr. 2011.

Q. Zhong and G. Weiss, "Synchroverter: Inverters that mimic synchronous generators," IEEE Transactions on Industrial Electronics, vol. 58, no. 4, pp. 1259-1267, Apr. 2011.

Q. Zhong, P. Nguyen, Z. Ma, and W. Sheng, "Self-synchronized Synchroverter: Inverters without a dedicated synchronization unit," IEEE Transactions on Transistors system, vol. 29, no. 2, pp. 617-630, 2014.

S. Debnath and M. Chinthavali, "Control of MMC-HVDC in low-inertia weak grids," in Proc. 2017 IEEE 12th International Conference on Transistors system and Drive Systems (PEDS), pp. 435-441.

S. Debnath and M. Chinthavali, "MMC-HVDC: Simulation and control system," in Proc. 2016 IEEE Energy Conversion Congress and Exposition (ECCE), pp. 1-8.

S. Debnath, J. Qin, B. Bahrani, M. Saeedifard, and P. Barbosa, "Operation, control, and applications of the modular multilevel converter: A review," IEEE Transactions on Transistors system, vol. 30, p. 37-53, Jan. 2015.

U. Tamrakar, D. Shrestha, M. Maharjan, BP Bhattarai, TM Hansen, and R. Tonkoski, "Virtual inertia: Current trends and future directions," Applied Sciences, vol. 7, no. 7, p. 654, 2017.

WECC Renewable Energy Modeling Task Force, "WECC Solar Plant Dynamic Modeling Guidelines," 2014.

Z. Shuai, W. Huang, C. Shen, J. Ge, and ZJ Shen, "Characteristics and restraining method of fast transient inrush fault currents in Synchroverter," IEEE Transactions on Industrial Electronics, vol. 64, no. 9, pp. 7487-7497, 2017.